analytical chemistry

Article

Cite This: Anal. Chem. 2019, 91, 10679−10686

pubs.acs.org/ac

Electrical and Label-Free Quantification of Exosomes with a Reduced Graphene Oxide Field Effect Transistor Biosensor

Yi Yu,[†] Yu-Tao Li,[†] Dan Jin,[†] Fan Yang,[†] Ding Wu,[†] Meng-Meng Xiao,[‡] Hong Zhang,*[,§] Zhi-Yong Zhang,*[,‡] and Guo-Jun Zhang*[,†]

[†]School of Laboratory Medicine, Hubei University of Chinese Medicine, 1 Huangjia Lake West Road, Wuhan 430065, People's Republic of China

[‡]Key Laboratory for the Physics and Chemistry of Nanodevices, Department of Electronics, Peking University, 5 Yiheyuan Road, Beijing 100871, People's Republic of China

[§]Teaching and Research Office of Forensic Medicine, Hubei University of Chinese Medicine, 1 Huangjia Lake West Road, Wuhan 430065, People's Republic of China

Supporting Information

ABSTRACT: Exosomes are small membrane-bound nanovesicles with a size of 50−150 nm which contain many functional biomolecules, such as nucleic acids and proteins. Due to their high homology with parental generation, they are of great significance in clinical diagnosis. At present, the quantitative detection of low concentrations of cancer-derived exosomes present in biofluids is still a great challenge. In this study, we develop an electrical and label-free method to directly detect exosomes with high sensitivity based on a reduced graphene oxide (RGO) field effect transistor (FET) biosensor. An RGO FET biosensor modified with specific antibody CD63 in the sensing area was fabricated and was used for electrical and label-free quantification of exosomes. The method achieved a low limit of detection down to 33 particles/μL, which is lower than that of many other available methods. In addition, the FET biosensor was employed to detect exosomes in clinical serum samples, showing significant differences in detecting healthy people and prostate cancer (PCa) patients. Different from other technologies, this study provides a unique technology capable of directly quantifying exosomes without labeling, indicating its potential as a tool for early diagnosis of cancer.

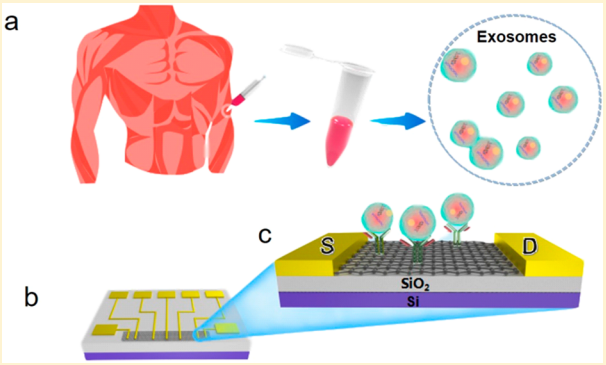

INTRODUCTION

The exosome (Exo) is a kind of microvesicle with a double phospholipid membrane structure with a diameter of 50−150 nm.[1] It is rich in protein, DNA, and miRNA and has extremely high homology, which has been found to play an important role in intercellular communication, metastasis, and angiogenesis.[2−4] Both normal cells and cancer cells can secrete exosomes, but cancer patients have more exosomes in their blood.[5] As the concentration of exosomes is related to the dynamics of some diseases, especially cancer, the quantitative detection of exosomes is helpful for the early analysis and diagnosis of diseases.[6] Exosomes are increasingly being recognized as promising circulating biomarkers of disease ("liquid biopsies").

In recent years, some methods have been applied to detect exosomes, such as nanoparticle tracking analysis (NTA),[7] flow cytometry,[8] Western blot,[9] and ELISA.[10,11] NTA can be used when the concentration of exosomes is between 10^7 and 10^9 particles/mL, and quantifications cannot be achieved when the concentration is lower than that. NTA is mainly used to detect ζ potential and particle size distribution. Flow cytometry can be used for high-throughput detection, but the scattered light of exosomes with particle sizes less than 100 nm is weak and cannot be accurately quantified. Western blot and ELISA analysis require large sample volumes, and both of them have limited sensitivity. Since tumor-derived exosomes in peripheral blood are limited in the early stage of cancer, it is difficult for the traditional quantitative detection methods to achieve early diagnosis of cancer due to their low sensitivity. In order to further improve the sensitivity, electrochemical methods,[12−16] fluorescenc,e[17−20] and microfluidic sensing[21−24] have been used for exosome quantification. Wang et al. used an electrochemical method to develop a nanotetrahedron-assisted aptasensor for direct capture of exosomes.[25] Im et al. detected exosomes on the basis of surface plasmon resonance transmitted through periodic nanopore arrays. Each array

Received: April 23, 2019
Accepted: July 23, 2019
Published: July 23, 2019

DOI: 10.1021/acs.analchem.9b01950
Anal. Chem. 2019, 91, 10679−10686

was functionalized with antibodies to analyze exosome surface proteins.[26] These methods can detect exosomes with high sensitivity, but they require complex interface engineering and a complicated nanofabrication process. Jin et al. used a fluorescence method to detect exosomes by employing graphene oxide nanosheets to adsorb single-stranded fluorescent aptamers and form a quenched nanoprobe to read out the presence of exosomes.[27] This method is convenient and suitable for clinical detection, but its sensitivity needs to be further improved. Moreover, the method requires fluorescent labeling. It is desirable to establish a highly sensitive, simple, economical, and convenient method for direct detection of exosomes.

As a label-free detection tool, a field effect transistor (FET) biosensor is one of the most promising biosensors in recent years. Through field effect transistors, microelectrical signals caused by the interactions between biomolecules on the sensing interface are transformed into readable electrical signals and amplified, with high sensitivity and good specificity.[28,29] Graphene-based FET biosensors have the advantages that include fast response, low detection limit, rapid detection, etc. To achieve high sensitivity, PNA instead of DNA was used as a probe molecule to realize DNA detection by using a RGO FET biosensor. A sensitivity as high as 100 fM was obtained. Moreover, the FET biosensor could be regenerated by denaturation and rehybridization.[30] Chen et al. used an aptamer-functionalized RGO FET biosensor to detect tobramycin within 5 s with a low detection limit down to 0.3 nM. The aptamer-functionalized RGO FET biosensors showed good stability and specificity.[31] Chen et al. also used an RGO FET biosensor functionalized by TEBAC to detect nitrates in water with high sensitivity and specificity. The response time was only 2−7 s, and the detection limit was as low as 1.1 μg/L.[32] In addition, graphene-based FET biosensors can also detect acetylcholine, dopamine, NO, and cell action potential.[33−36] However, the detection of exosomes using FET biosensors has not yet been reported.

CD63 is a protein that has been demonstrated to exist abundantly on the surface of exosomes. It is a marker that distinguishes exosomes from other vehicles, such as microvesicles and apoptotic bodies. It has been reported that CD63 antibody can be used to capture exsomes for the early diagnosis of cancer.[37,38] For instance, Kanwar et al. used a CD63-functionalized exosome microfluidic chip to distinguish cancer patients from healthy patients, in which the results showed that serum exosomes in cancer patients were higher than those in healthy patients.[39] Zhou et al. modified a specific aptamer on the electrode surface to recognize CD63 protein on the exosome surface for the purpose of identifying exosomes.[40] In this work, we explore a CD63-functionalized reduced graphene oxide (RGO) FET biosensor that can be used to directly quantify exosomes in a label-free and sensitive manner, as illustrated in Figure 1. The FET device is fabricated by standard semiconductor technology, after which graphene is drop-casted onto the sensing channel of the device. Subsequently, CD63 antibody is functionalized on the RGO FET device. Exosome is thus detected by the CD63-functionalized FET biosensor via specific binding between CD63 antibody and CD63 on the surface of exosomes. It is shown that this method can be used for the accurate quantification of exosomes, providing a new platform for early disease diagnosis.

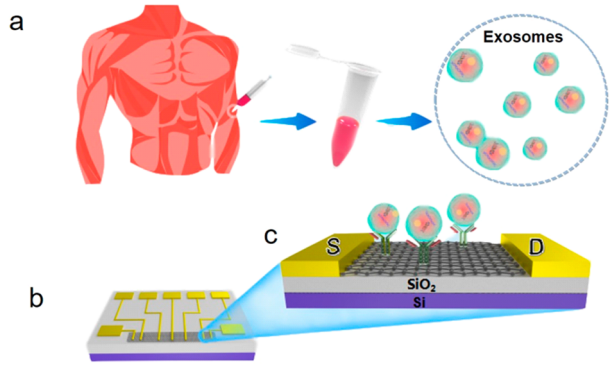

Figure 1. Schematic diagram of a CD63 antibody functionalized RGO FET biosensor for detection of exosomes. (a) Exosomes are isolated and purified from the blood of patients. (b) RGO FET biosensor. (c) After anti-CD63 functionalization in the sensing region, exosomes can be directly bound to the CD63 antibody functionalized RGO FET biosensor for electrical and label-free detection.

EXPERIMENTAL SECTION

Materials and Chemicals. 1-Pyrenebutanoic acid succinimidyl ester (PASE) and bovine serum (BSA) were purchased from Sigma-Aldrich (Shanghai, China). Graphene oxide (GO) powder (99.99995%) was purchased from Alfa Aesar Co. Ltd. (Tianjin, China). Cy-5 NHS ester was purchased from Bioorth Biotech Co. Ltd. (Nanjing, China). Hydrazine (98%) was purchased from Generay Biotech Co. Ltd. (Shanghai, China). Streptavidin (SA) was purchased from Solarbio Science & Technology Co. Ltd. (Beijing, China). Anti-CD63 was purchased from Abcam (Cambridge, U.K.). Anti-BNP, LCN-2, glutaraldehyde, and phosphotungstic acid were purchased from Sigma-Aldrich (Shanghai, China). The cell culture medium RPMI-1640 was purchased from Thermo Fisher Scientific (Waltham, U.K.). Human cell line liver cancer HepG2 was obtained from the American Type Culture Collection. Ultrapure water was obtained from a Millipore water purification system (18.2 MΩ.cm resistivity, Milli-Q Direct 8). Serum samples were provided by Hubei provincial people's hospital, Wuhan, China. All of the chemicals used in this study were of analytical grade. All other chemicals unless specified were reagent grade and were used without further purification.

Fabrication of RGO FET Biosensors. The RGO FET biosensor was fabricated as previously reported. Briefly, an RGO solution was prepared by a chemical reduction method. A 0.2 μL portion of 0.2 mg/mL RGO solution was drop-casted on the sensing channel of the chip and thermally annealed at 80 °C in a vacuum oven for 2 h. In order to obtain graphene with a thinner layer, the chip was sonicated with Pirahna solution (7/3 v/v concentrated H_2SO_4/35% H_2O_2). Finally, the chip was rinsed with deionized water three times and was dried with nitrogen for subsequent experiments.

Surface Functionalization. To modify the CD63 antibody on the chip, 0.5 mM PASE was first incubated with the RGO FET chip at room temperature for 1.5 h. The chip was then washed with DMSO, ethanol, and pure water, respectively, and then dried with nitrogen. PASE was fixed on the RGO surface though $\pi-\pi$ stacking interactions between the pyrene group and the graphene surface. PASE provides the succinimidyl ester group on the other end for covalently binding to the amino group on the antibody. CD63 antibodies (100 μg/mL) were introduced onto the chip for incubation at

DOI: 10.1021/acs.analchem.9b01950
Anal. Chem. 2019, 91, 10679−10686

room temperature for 1.5 h. Then the chip was washed with PBS and pure water, respectively, and then dried with nitrogen. Finally, 1 mg/mL BSA was used to prevent nonspecific adsorption.

Exosome Purification. HepG2 was cultured with RPMI-1640 medium, which contained 10% (v/v) FBS, 1% (v/v) penicillin, and 100 μg/mL streptomycin, and maintained under a humidified atmosphere of 5% CO_2 at 37 °C. The cells were collected after being cultured for 48 h in a serum-free medium. Subsequently, exosomes were purified according to the steps of standard overspeed centrifugation. The centrifugation method was as follows: the sample was first centrifuged at 300*g* for 15 min in order to remove impurities such as cell fragments, and then the supernatant was centrifuged at 2000*g* for 20 min to remove the cell debris. The filtrate was collected, filtered with a 0.22 μm filter membrane (Millipore), and centrifuged at 1000*g* for 30 min. Finally, the supernatant solution was centrifuged at 110000*g* for 70 min to precipitate exosomes. In order to obtain higher purity exosomes, the exosomes were recentrifuged after resuspension (11000*g*, 70 min). Finally, the exosome pellet was resuspended in 400 μL of PBS and stored at −80 °C for use.

Exosome Detection. Exosomes with the appropriate concentration (10 μL) were incubated with the antibody-functionalized RGO FET at 37 °C for 30 min. The chip was then rinsed with PBS and pure water to wash unbound exosomes away. Finally, the chip was dried with nitrogen.

Exosome Detection in Serum. To verify the potential applications of the RGO FET biosensor in clinical practice, clinical samples were tested with the CD63-functionalized RGO FET biosensor. Clinical blood samples were taken from the people's hospital of Hubei province, which was approved by the Ethics Committee of Renmin Hospital. The practical serum samples involved six patients with pancreatic cancer and eight normal patients as control. Exosomes were purified by the overspeed centrifugation method mentioned in previous literature.[27] Exosome detection in clinical serum samples was performed as described above.

Electrical Measurements. The measurement system consisting of a probe station (EverBeing BD-6) and a semiconductor characterization system (Keithley 4200-SCS) was used. All measurements regarding the electrical characterization of the FET devices were conducted with a liquid gate at room temperature. When the different concentrations of exosomes were conjugated with the antibodies on the chip, the electrical transfer curves including I_d−V_g (I_d is drain current, and V_g is gate voltage) were recorded.

Characterization of Exosomes. *TEM Observation.* First, 15 μL of the exosome suspension was loaded in the 400 mesh carbon-coated copper grid and fixed with 2% glutaraldehyde. The grid was stained with 2% phosphotungstic acid for 10 min and then washed twice with PBS. After drying at room tempreture, the grid was observed under a transmission electron microscope (TEM) (JEM-2100, Japan) at 80 kV.

NTA Analysis. Nanoparticle tracking analysis (NTA) can characterize exosomes suspended in liquids. A 20 μL portion of exosomes was diluted 100-fold with PBS and then filtered with a 0.22 μm filter membrane. When the sample was irradiated by the laser in NTA, scattered light signals caused by the Brownian motion of nanoparticles were collected by an optical microscope and CMOS camera. The concentration and particle size distribution of exosomes were measured by NTA (Zeta view Ltd., Germany) under optimal parameter settings.

SEM Observation. Exosomes were incubated on the CD63-functionalized FET chip at 37 °C for 30 min, after which unbound exosomes were subsequently washed off with PBS. The exosomes were then fixed with 2.5% glutaraldehyde and finally dehydrated by gradient with ethanol. Platinum nanoparticles were then coated with a sputter coater (208HR, Cressington Scientific Instruments, USA) to enhance the electrical conductivity of biological samples. Finally, the chip was observed under a scanning electron microscope (SEM) (ZeissSIGMA, Germany) at 5 kV.

Western Blot. Exosomes were lysed in a buffer containing protease inhibitors, and protein quantification was performed with a BCA Protein Assay Kit (Beyotime Biotechnology Co. Ltd., Shanghai, China). Proteins were denatured and separated by gel electrophoresis, transferred to a polyvinylidene fluoride membrane (PVDF) after cooling to room temperature, and then blocked with 5% (w/v) bovine albumin in TBST for 2 h. Blots were further inmmunoblotted with primary antibodies against CD63 (SanYing, 1:500 solution), CD9 (SanYing, 1:500 solution), and Tsg-101 (SBI, 1:500 solution) overnight at 4 °C. Subsequently, the blots were incubated with HRP-conjugated secondary antibody (1:50000 solution) at 37 °C for 2 h. Finally, the membranes were washed three times with TBST. The signal was obtained by a Gel Imaging System (Thermo Fisher, USA).

RESULTS AND DISCUSSION

Detection Principle. The principle of the RGO FET biosensor for detecting exosomes is shown in Figure S1. As illustrated, the FET device is fabricated on a SiO_2/Si substrate by the conventional macro-nano processing technologies. Subsequently, PASE is fixed on the RGO surface through π−π stacking interactions between the pyrene group and the graphene surface. The antibody is then covalently immobilized on the FET surface by a reaction between the amino group on anti-CD63 and the succinimidyl ester group on the other end of the PASE. BSA is used for blocking the unreacted aldehyde groups to prevent nonspecific adsorption. Finally, when the exosomes are captured by the specific antibody, the net carrier density on the chip surface changes due to a contribution of the negative charges of the exosomes, resulting in the left shift of the Dirac point.

Characterization of Exosomes. Exosomes were isolated and purified from liver cancer cells (HepG2) by multiple steps of ultracentrifugation. Standard characterization of exosomes was performed using TEM, NTA, and Western blot. As shown in Figure 2a, it is seen from the TEM image that the exosomes had a complete phospholipid bilayer structure and a typical cup shape with particle sizes between 30 and 120 nm. The morphology is consistent with that of the typical exosomes reported in the literature.[41] The relation between particle size and relative concentration could be determined by NTA analysis. It can be seen that the purified exosomes mainly had a size of around 120 nm (Figure 2b). The concentration of the collected exosomes was 3.3×10^{10} particles/mL (Figure S2a). In our experiment, CD63 antibody, a transmembrane 4 superfamily member, was selected for capturing exosomes. Western blot was used to detect general exosome markers: CD63, CD9, and Tsg-101. Figure S2b shows the ζ potential distribution on the surface of the exosome. It can be found that the average potential on the surface of the exosome was −37.5 mV, proving that the surface of the exosome contains negative charges. From the detection results of Figure 2c, it can be seen

DOI: 10.1021/acs.analchem.9b01950
Anal. Chem. 2019, 91, 10679−10686

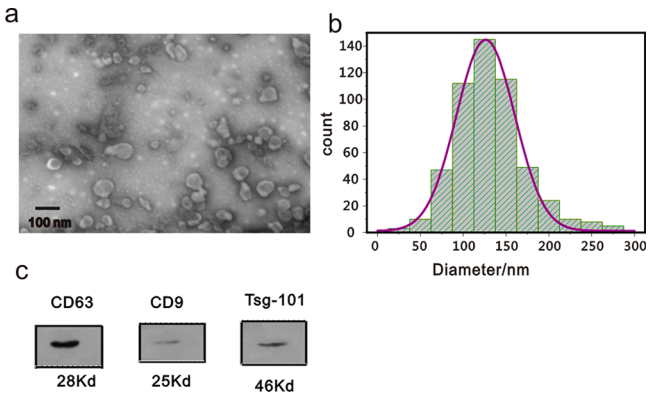

Figure 2. Characterization of exosomes: (a) TEM image of exosomes with double-wall lipid membrane layers ranging approximately 30−150 nm in diameter; (b) size distribution of exosomes by NTA analysis; (c) expression of CD63 (the exosomal marker), CD9, and Tsg-101 in exosomes.

that these three proteins existed in exosomes, among which CD63 was the most abundant. Therefore, it is feasible to use CD63 antibody to capture exosomes in this study. The above experimental results show that exosome purification was successful.

Surface Functionalization and Exosome Capture. In order to prove that the modification process of anti-CD63 on the RGO surface was successful, a fluorescence experiment was performed by labeling CD63 antibody with a Cy-5 fluorescent dye, dropping the Cy-5 labeled CD63 antibody on a silicon chip, and visualizing the fluorescent spot by a fluorescence microscope. The Cy-5 fluorescent dye was diluted to 1 μg/mL and mixed with CD63 antibody at the same volume for 30 min at room temperature. The labeling was completed by binding of Cy-5 NHS ester to the amino groups of the antibody. Before the labeled Cy-5 was applied to the silicon surface, it was modified with RGO and PASE in advance as mentioned above. The labeled antibody was dropped on the silicon chip and observed under a fluorescence microscope. It can be seen that an obvious fluorescence signal was obtained in Figure 3a, indicating that CD63 antibody was successfully modified on the RGO surface. Nevertheless, in the case of a control experiment, in which the chip was not modified with antibody, but only Cy-5 was added, only a negligible fluorescence signal was determined, as shown in Figure 3b. It may be caused by uneluted fluorescence dye and nonspecific adsorption. Therefore, it is indicated that the fluorescence signal in Figure 3a completely comes from the CD63 antibody immobilization on the chip.

To confirm the successful functionalization of anti-CD63 on the FET chips, an atomic force microscope (AFM) before and after anti-CD63 immobilization on the RGO FET biosensor was employed to study the morphology and structure of the RGO FET device. As observed in Figure S3, the height difference after RGO modification was estimated to be 1.3−5.8 nm. The binding of anti-CD63 to the RGO surface led to a height increase to 12.6−21.1 nm. According to literature reports,[42] the size of the antibody is about 10−15 nm. The results indicate that the height increase is caused by binding of anti-CD63 to the RGO FET biosensor as anticipated.

The I_d−V_g characteristic curves in Figure 3c represent the stepwise process of antibody modification and exosome capture by the FET sensors. After PASE was modified, the

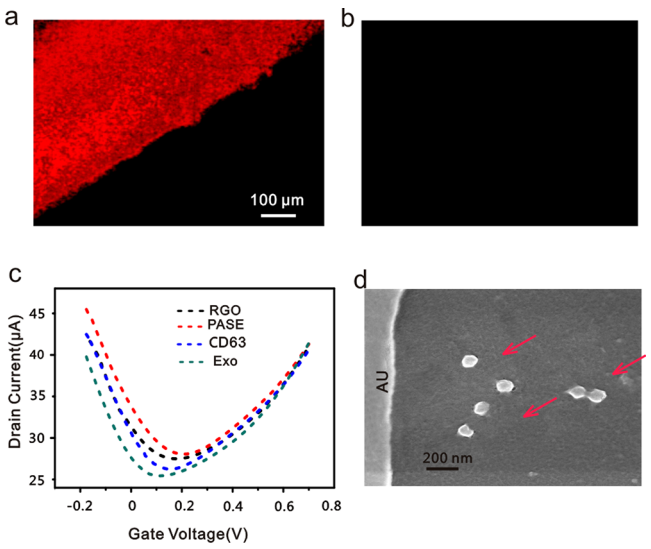

Figure 3. (a) Fluorescence microscope image of Cy-5 fluorophore labeled CD63 antibody modified on a silicon chip. (b) Fluorescence microscope image of a silicon chip without CD63 modification. (c) I_d−V_g curves of the stepwise functionalization process of the FET device including RGO assembly, PASE modification, CD63 antibody immobilization, and exosome binding, respectively. (d) SEM image of exosomes captured by the immobilized CD63 antibody in sensing channel.

Dirac point shifted to the right. As described in a previous report, the reduced graphene oxide FET biosensor is a p-type device.[43] PASE provides positive charges to introduce p-doping into the graphene,[44] leading to the right-shifted Dirac point. When the anti-CD63 was bound to the graphene surface, the contribution of the negatively charged CD63 antibody led to the increase of surface charge density and induced n-doping, shifting the Dirac point to the left. After 3×10^8 particles/mL exosomes were added onto the antibody-modified FET sensor, specific binding between anti-CD63 and exosomes occurred. Due to the contribution of exosome negative charges, n-type doping took place on the device, leading to the left shift of the Dirac point. Therefore, the I_d−V_g characteristic curves again indicate that anti-CD63 was modified on the FET chip and exosomes were successfully captured by the anti-CD63-modified FET chip.

To further verify that exosomes were bound the RGO FET chip surface, SEM was employed to visualize the exosomes inside the sensing channel after exosomes were applied to the CD63-modified FET sensor. It can be intuitively seen in Figure 3d that exosomes were visible inside the sensing channel between source and drain. The sizes of the exosomes were all around about 100 nm, and the edges of the exosomes had obvious membrane structure characteristics. Therefore, it is further demonstrated that exosomes have been localized on the FET biosensor as anticipated.

Sensitivity. In order to test the sensitivity of the RGO FET biosensor for exosome detection, exosomes were diluted into different concentrations and applied to the anti-CD63-functionalized FET device from 3.3×10^4 particles/mL to 3.3×10^9 particles/mL. As shown in Figure 4a, the Dirac point shifted to the left as the concentration of exosomes increased during the detection. With the increase of exosome concentrations, the observed $-\Delta V_{CNP}$ (12, 22, 32, 44, 56, and 68 mV, respectively, corresponding to the aforementioned

DOI: 10.1021/acs.analchem.9b01950
Anal. Chem. 2019, 91, 10679−10686

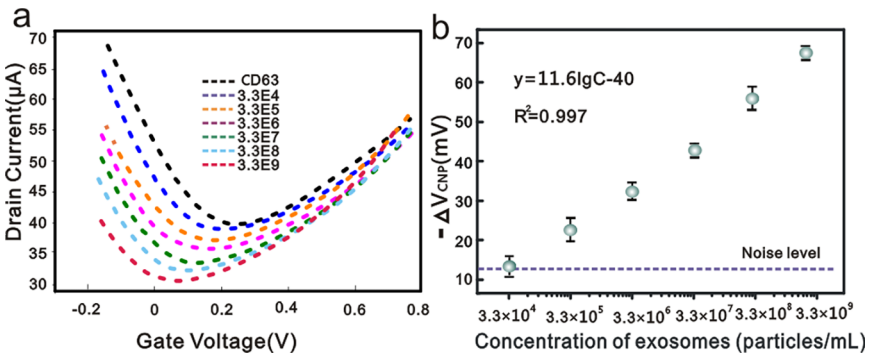

Figure 4. Electrical response of the RGO FET biosensor to different concentrations of exosomes. (a) Transfer curves of the RGO FET biosensor interacting with varying concentrations of exosomes. (b) Shift of V_{CNP} of the RGO FET biosensor at a series of exosome concentrations. The dashed line represents the signal/noise ratio of 3 from the blank control test.

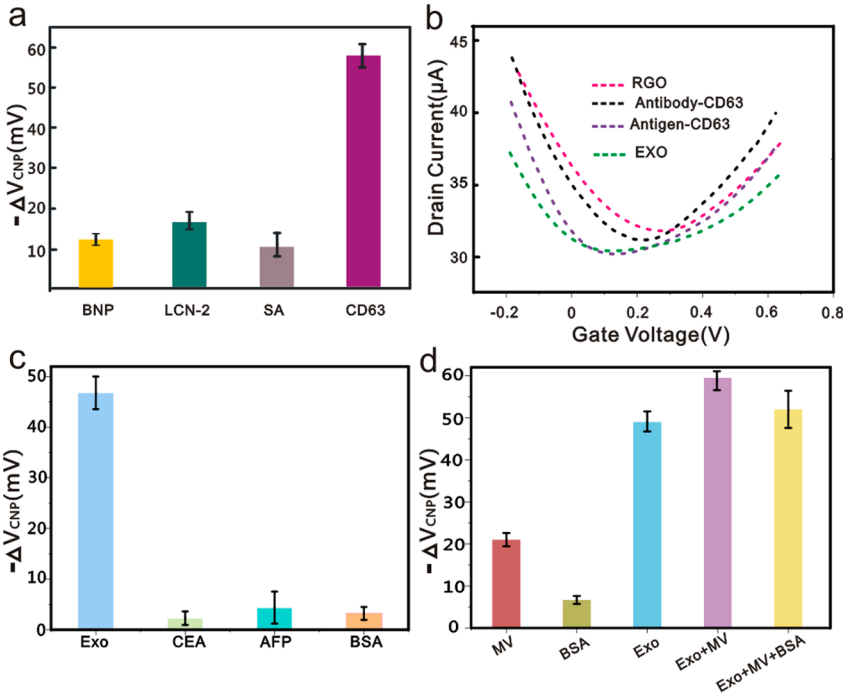

Figure 5. Specificity study. (a) Changes in the Dirac point after BNP, LCN-2, and strepavidin were respectively modified on the chip and interacted with exosomes. (b) I_d–V_g curves of the RGO FET biosensor undergoing RGO assembly, antibody immobilization, binding of CD63 with antibody, and introduction of exosomes, respectively. (c) Dirac point changes after CEA, AFP, BSA, and exosomes were applied onto the chip, respectively. (d) Dirac point changes of the anti-CD63 immobilized RGO FET biosensor interacting with different substances.

concentrations from low to high, respectively) increased gradually. As the concentration of exosomes captured by the FET biosensor increased, the net carrier density on the surface of the FET sensor increased, generating an n-doping on the device and finally shifting the Dirac point to the left. With an increase in exosome concentration, the current also decreased in addition to the Dirac point shift. As the RGO FET is a p-type device, it is mainly for hole conduction.[35] It is clear that the current gradually decreases with a gradual increase in exosome concentrations because the exosome is negatively charged. The results are consistent with those reported in other literature.[30,45] Figure 4b shows a linear relationship between exosome concentration and changes in the Dirac point (ΔV_{CNP} = $V_{CNP\ after\ incubation}$ − $V_{CNP\ before\ incubation}$). In response, a regression equation is expressed as $-\Delta V_{CNP} = 11.6 \log C - 40$, where C is the exosome concentration, and a correlation coefficient value (R^2) of 0.997 is obtained. It can be seen that the signal to noise level is 12 mV (S/N ratio 3). On the basis of the signal that exceeds the baseline by 3-fold, the LOD was found to be 33 particles/μL. Usually, it is reported that the content of exosomes in human blood is 10^2–10^8 particles/μL.[46] The LOD of this method is lower than the normal concentration of exosomes in the human body, indiacting that the RGO FET biosensor achieved a high sensitivity.

Many detection methods have been employed for detecting exosomes. For example, Zhou et al. used an electrochemical method to detect exosomes on the basis of aptamers with a sensitivity of 10^3 particles/μL.[40] Doldan et al. used an electrochemical sandwich immunosand which assay to detect exosomes down to 2×10^2 particles/μL.[47] Dong et al. used aptamer–magnetic bead bioconjugates to capture tumor exosomes derived from LNCaP cells. Under the optimal conditions, a detection limit down to 70 particles/μL was

DOI: 10.1021/acs.analchem.9b01950
Anal. Chem. 2019, 91, 10679–10686

obtained.[48] Jin et al. used graphene oxide with target-responsive aptamers to profile exosomal markers. This assay achieved a detection limit down to 1.6×10^2 particles/μL.[27] Wang et al. developed an electrochemical method based on nanotetrahedral-assisted aptasensors for label-free detection of exosomes, with a sensitivity as high as 20 particles/μL.[25] The performance comparison between this work and other works is summarized in Table S1. It is clear that the performance of the FET biosensor is superior to that of many other methods. Moreover, the developed assay is capable of directly detecting exosomes without labeling.

Specificity. In order to study the specificity of the FET biosensor, different kinds of antibodies were immobilized on the FET chip and the same concentration of the exosomes was interacted with the various antibody-immobilized FET chips. In addition to modifying CD63 antibodies on the FET biosensor, the following nonspecific antibodies were also modified on different FET chips: anti-BNP, LCN-2, and streptavidin, respectively. As shown in Figure 5a, negligible ΔV_{CNP} change was observed after exosomes were applied to the nonspecific antibody (anti-BNP, LCN-2, and streptavidin, respectively) functionalized RGO FET biosensor. The $-\Delta V_{CNP}$ values were found to be 12, 15, and 9 mV, respectively. Nevertheless, the $-\Delta V_{CNP}$ value was 59 mV for the case where exosomes were introduced to the CD63 antibody functionalized FET biosensor. This indicates that anti-CD63 can specifically recognize exosomes on the sensor chip.

To verify that the binding between exosomes and CD63 antibody is caused by the specific interaction of the surface antigen of exosomes with CD63 antibody, the CD63-functionalized RGO FET biosensor was first interacted with CD63 antigen and then incubated with exosomes. The I_d–V_g curves of the RGO FET biosensor undergoing RGO assembly, antibody immobilization, binding of CD63 with antibody, and introduction of exosomes, respectively, are shown in Figure 5b. As can be seen, the left shift of Dirac point occurred after immobilization of antibody on the RGO FET biosensor, as discussed earlier. The Dirac point shifted to the left again after CD63 was bound to the immobilized CD63 antibody. This is because CD63 (pI 6.79) is negatively charged in pH 7.4 PBS solution.[49] After the exosomes were finally applied to the FET surface, the Dirac point barely shifted. The possible reason is that almost all binding sites are occupied by CD63 antigen, resulting in the inability of exosomes to bind to CD63 antibody. This indicates that exosomes are specifically bound to CD63 antibodies immobilized on the FET biosensor.

To further investigate the specificity of the FET biosensor, the anti-CD63-functionalized FET biosensor was used to detect 10 μg/mL of nonspecific protein CEA, BSA, and AFP, respectively, and 100 ng/mL of exosomes. As shown in Figure 5c, the Dirac point changes were almost negligible when nonspecific proteins such as CEA, APF, and BSA were detected. Meanwhile, the signal was significantly enhanced when exosomes were applied for detection. In addition, exosomes (10^6 particles/mL), 4% BSA, MVs (10^8 particles/mL), and their mixtures (Exo + MVs and Exo + MVs + BSA) were applied to the anti-CD63-functionalized RGO FET, respectively. The corresponding results are shown in Figure 5d. It was observed that the $-\Delta V_{CNP}$ values were 21 and 13 mV, respectivel, when nonspecific MVs and BSA were interacted with the biosensor. The $-\Delta V_{CNP}$ value was 48 mV when exosomes were interacted with the biosensor. In the case of mixtures, it was found that the $-\Delta V_{CNP}$ values were 56 and 52 mV, respectively, when the mixtures (Exo + MVs and Exo + MVs + BSA) were respectively applied to the biosensor. The results are consistent with previous reports.[27] It can be concluded that this biosensor can detect exosomes with high specificity.

Clinical Sample Analysis. In order to further verify the application ability of the FET biosensor in real samples, we collected the blood serum samples of six prostate cancer patients as the experimental group and the blood serum samples of eight normal patients as the control group and applied these serum samples to the anti-CD63-modified RGO FET sensor. In the serum samples provided by each patient, we took an equal volume of serum to extract exosomes and purified exosomes according to the method described above. TEM images of exosomes extracted from serum are shown in Figure S4. The image showed that an exosome with a particle size of about 100 nm was similar to that in liver cancer cells with obvious cup-dish lipid membrane structure. After collection of exosomes from each sample, the serum was applied to the CD63-functionalized RGO FET biosensor. As can be seen from Figure 6, fewer exosomes were found in the serum of normal people in comparison to those in the serum of pancreatic cancer patients. The level of exosomes in patients with prostate cancer was higher than that in normal people. Statistically, significant differences were found between the two groups ($P < 0.01$). Thus, this reveals that the fabricated RGO FET biosensor is able to differentiate exosome levels in cancer patients and normal people, indicating its potential as a label-free sensing tool for cancer diagnosis.

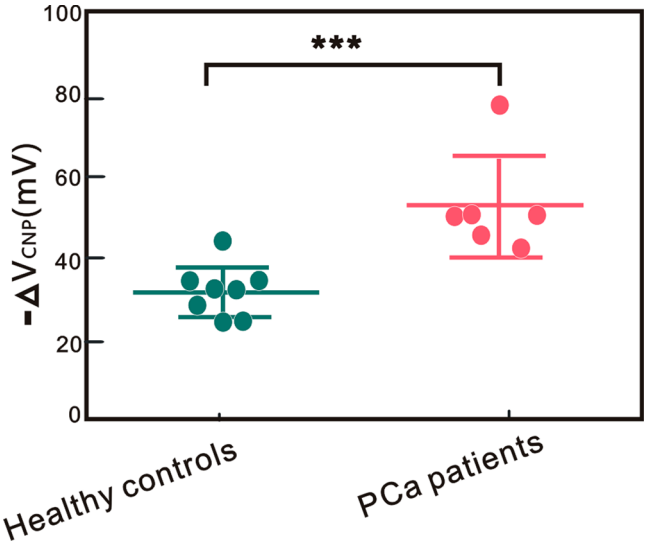

Figure 6. Expression level of exosomes in the serum obtained from healthy volunteers and cancer patients.

Reusability. After detection, the exosome-bound FET biosensor was treated with highly concentrated salt solutions (NaCl, 1 M) to dissociate the binding between exosomes and the anti-CD63. Then, exosomes (10^8 particles/mL) were applied to the anti-CD63-functionalized FET biosensor once more, followed by dissociation. As such, three cycles were conducted by repeating the process of dissociation and binding. The changes in Dirac point undergoing the three cycles are shown in Figure 7. In each process of dissociation and binding, the changes in Dirac point were found to be 52,

DOI: 10.1021/acs.analchem.9b01950
Anal. Chem. 2019, 91, 10679−10686

45, and 38 mV, respectively. This indicates that the FET biosensor can be reused.

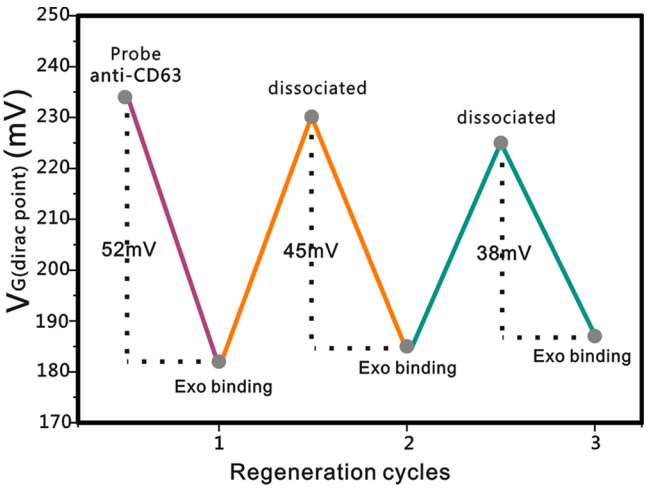

Figure 7. Reusability study of the FET biosensor for exosome detection. The concentrations of exosomes and NaCl were 10^8 particles/mL and 1 M, respectively.

CONCLUSIONS

To sum up, we have developed a CD63 antibody functionalized RGO FET biosensor for electrical and label-free detection of exosomes with high sensitivity and specificity. This method has the following advantages. (i) Different from the existing methodologies, the detection method is direct and label-free. (ii) Sensitivity as high as 33 particles/μL is achieved, which is higher than that of many other methods. (iii) Significant differences in exosome levels in serum between prostate cancer patients and normal people is found by the assay, showing a clinical application potential. (iv) This method is also universal, meaning that exosomes from different tumors are detectable by changing different antibodies in a specific manner. This method provides a new platform for the detection of exosomes and is expected to be used in clinical practice in the future.

ASSOCIATED CONTENT

Supporting Information

The Supporting Information is available free of charge on the ACS Publications website at DOI: 10.1021/acs.analchem.9b01950.

Additional information on the schematic diagram of exosome detection by a CD63-modified FET biosensor, exosome characterization, AFM image before and after anti-CD63 modification, TEM image of exosome purified from serum, and a comparison of different exosome detection techniques (PDF)

AUTHOR INFORMATION

Corresponding Authors

*H.Z.: e-mail, redguo@hotmail.com.
*Z-Y.Z.: e-mail, zyzhang@pku.edu.cn.
*G.-J.Z.: tel, +86-27-68890259; fax, +86-27-68890259; e-mail, zhanggj@hbtcm.edu.cn.

ORCID

Fan Yang: 0000-0002-8490-4183
Zhi-Yong Zhang: 0000-0003-1622-3447
Guo-Jun Zhang: 0000-0001-9096-9226

Notes

The authors declare no competing financial interest.

ACKNOWLEDGMENTS

This work was supported by the National Natural Science Foundation of China (No. 21675041).

REFERENCES

(1) Tkach, M.; Thery, C. *Cell* **2016**, *164*, 1226−1232.
(2) Azmi, A. S.; Bao, B.; Sarkar, F. H. *Cancer Metastasis Rev.* **2013**, *32*, 623−642.
(3) Zhang, K.; Zhao, X.; Chen, X.; Wei, Y.; Du, W.; Wang, Y.; Zhao, Q. *ACS Appl. Mater. Interfaces* **2018**, *10*, 30081−30091.
(4) Fang, X.; Duan, Y.; Adkins, G. B.; Pan, S.; Wang, H.; Liu, Y.; Zhong, W. *Anal. Chem.* **2018**, *90*, 2787−2795.
(5) Liu, C.; Zhao, J.; Tian, F.; Cai, L.; Zhang, W.; Feng, Q.; Cong, Y. *Nat. Biomed. Eng.* **2019**, *3*, 183.
(6) Melo, S. A.; Luecke, L. B.; Kahlert, C.; Fernandez, A. F.; Gammon, S. T.; Kaye, J.; Reissfelder, C. *Nature* **2015**, *523*, 177.
(7) Sokolova, V.; Ludwig, A. K.; Hornung, S.; Rotan, O.; Horn, P. A.; Epple, M.; Giebel, B. *Colloids Surf., B* **2011**, *87*, 146−150.
(8) Van Der Pol, E.; Hoekstra, A. G.; Sturk, A.; Otto, C.; Van Leeuwen, T. G.; Nieuwland, R. *J. Thromb. Haemostasis* **2010**, *8*, 2596−2607.
(9) Nolte, E. N.; van der Vlist, E. J.; Aalberts, M.; Mertens, H. C.; Bosch, B. J.; Bartelink, W.; Wauben, M. H. *Nanomedicine* **2012**, *8*, 712−720.
(10) Alvarez, M. L.; Khosroheidari, M.; Ravi, R. K.; DiStefano, J. K. *Kidney Int.* **2012**, *82*, 1024−1032.
(11) Jorgensen, M. M.; Bæk, R.; Varming, K. *J. Extracell. Vesicles* **2015**, *4*, 26048.
(12) Sánchez-Tirado, E.; Salvo, C.; González-Cortés, A.; Yáñez-Sedeño, P.; Langa, F.; Pingarrón, J. M. *Anal. Chim. Acta* **2017**, *959*, 66−73.
(13) Jeong, S.; Park, J.; Pathania, D.; Castro, C. M.; Weissleder, R.; Lee, H. *ACS Nano* **2016**, *10*, 1802−1809.
(14) Zhou, Y. G.; Mohamadi, R. M.; Poudineh, M.; Kermanshah, L.; Ahmed, S.; Safaei, T. S.; Kelley, S. O. *Small* **2016**, *12*, 727−732.
(15) Boriachek, K.; Umer, M.; Islam, M. N.; Gopalan, V.; Lam, A. K.; Nguyen, N. T.; Shiddiky, M. J. *Analyst* **2018**, *143*, 1662−1669.
(16) Liang, K.; Liu, F.; Fan, J.; Sun, D.; Liu, C.; Lyon, C. J.; Koay, E. J. *Nat. .Biomed. Eng.* **2017**, *1*, 0021.
(17) Lewis, J. M.; Vyas, A. D.; Qiu, Y.; Messer, K. S.; White, R.; Heller, M. J. *ACS Nano* **2018**, *12*, 3311−3320.
(18) He, F.; Wang, J.; Yin, B. C.; Ye, B. C. *Anal. Chem.* **2018**, *90*, 8072−8079.
(19) Zhang, Q.; Wang, F.; Zhang, H.; Zhang, Y.; Liu, M.; Liu, Y. *Anal. Chem.* **2018**, *90*, 12737−12744.
(20) Yang, Y.; Kannisto, E.; Yu, G.; Reid, M. E.; Patnaik, S. K.; Wu, Y. *ACS Appl. Mater. Interfaces* **2018**, *10*, 43375−43386.
(21) Zhang, P.; He, M.; Zeng, Y. *Lab Chip* **2016**, *16*, 3033−3042.
(22) Xu, H.; Liao, C.; Zuo, P.; Liu, Z.; Ye, B. C. *Anal. Chem.* **2018**, *90*, 13451−13458.
(23) Zhao, Z.; Yang, Y.; Zeng, Y.; He, M. *Lab Chip* **2016**, *16*, 489−496.
(24) Dolatmoradi, A.; Mirtaheri, E.; El-Zahab, B. *Lab Chip* **2017**, *17*, 1332−1339.
(25) Wang, S.; Zhang, L.; Wan, S.; Cansiz, S.; Cui, C.; Liu, Y.; Wu, Y. *ACS Nano* **2017**, *11*, 3943−3949.
(26) Im, H.; Shao, H.; Park, Y. I.; Peterson, V. M.; Castro, C. M.; Weissleder, R.; Lee, H. *Nat. Biotechnol.* **2014**, *32*, 490.
(27) Jin, D.; Yang, F.; Zhang, Y.; Liu, L.; Zhou, Y.; Wang, F.; Zhang, G. J. *Anal. Chem.* **2018**, *90*, 14402−14411.
(28) Song, Y.; Luo, Y.; Zhu, C.; Li, H.; Du, D.; Lin, Y. *Biosens. Bioelectron.* **2016**, *76*, 195−212.

DOI: 10.1021/acs.analchem.9b01950
Anal. Chem. 2019, 91, 10679−10686

(29) Mao, S.; Chang, J.; Pu, H.; Lu, G.; He, Q.; Zhang, H.; Chen, J. *Chem. Soc. Rev.* **2017**, *46*, 6872−6904.
(30) Cai, B.; Wang, S.; Huang, L.; Ning, Y.; Zhang, Z.; Zhang, G. J. *ACS Nano* **2014**, *8*, 2632−2638.
(31) Chen, X.; Liu, Y.; Fang, X.; Li, Z.; Pu, H.; Chang, J.; Mao, S. *Biosens. Bioelectron.* **2019**, *126*, 664−671.
(32) Chen, X.; Pu, H.; Fu, Z.; Sui, X.; Chang, J.; Chen, J.; Mao, S. *Environ. Sci.: Nano* **2018**, *5*, 1990−1999.
(33) Hess, L. H.; Lyuleeva, A.; Blaschke, B. M.; Sachsenhauser, M.; Seifert, M.; Garrido, J. A.; Deubel, F. *ACS Appl. Mater. Interfaces* **2014**, *6*, 9705−9710.
(34) He, Q.; Sudibya, H. G.; Yin, Z.; Wu, S.; Li, H.; Boey, F.; Zhang, H. *ACS Nano* **2010**, *4*, 3201−3208.
(35) Xie, H.; Li, Y. T.; Lei, Y. M.; Liu, Y. L.; Xiao, M. M.; Gao, C.; Zhang, G. J. *Anal. Chem.* **2016**, *88*, 11115−11122.
(36) Cohen-Karni, T.; Qing, Q.; Li, Q.; Fang, Y.; Lieber, C. M. *Nano Lett.* **2010**, *10*, 1098−1102.
(37) Theodoraki, M. N.; Yerneni, S. S.; Hoffmann, T. K.; Gooding, W. E.; Whiteside, T. L. *Clin. Cancer Res.* **2018**, *24*, 896−905.
(38) Boriachek, K.; Islam, M. N.; Gopalan, V.; Lam, A. K.; Nguyen, N. T.; Shiddiky, M. J. *Analyst* **2017**, *142*, 2211−2219.
(39) Kanwar, S. S.; Dunlay, C. J.; Simeone, D. M.; Nagrath, S. *Lab Chip* **2014**, *14*, 1891−1900.
(40) Zhou, Q.; Rahimian, A.; Son, K.; Shin, D. S.; Patel, T.; Revzin, A. *Methods* **2016**, *97*, 88−93.
(41) Théry, C.; Amigorena, S.; Raposo, G.; Clayton, A. *Curr. Protoc. Cell Biol.* **2006**, *30*, 3.22.1.
(42) Ono, T.; Kanai, Y.; Inoue, K.; Watanabe, Y.; Nakakita, S. I.; Kawahara, T.; Matsumoto, K. *Nano Lett.* **2019**, *19*, 4004−4009.
(43) Zhang, C.; Xu, J. Q.; Li, Y. T.; Huang, L.; Pang, D. W.; Ning, Y.; Zhang, G. J. *Anal. Chem.* **2016**, *88*, 4048−4054.
(44) Hao, Z.; Zhu, Y.; Wang, X.; Rotti, P. G.; DiMarco, C.; Tyler, S. R.; Lin, Q. *ACS Appl. Mater. Interfaces* **2017**, *9*, 27504−27511.
(45) Zheng, C.; Huang, L.; Zhang, H.; Sun, Z.; Zhang, Z.; Zhang, G. J. *ACS Appl. Mater. Interfaces* **2015**, *7*, 16953−16959.
(46) Wang, Y.; Yuan, W.; Kimber, M.; Lu, M.; Dong, L. *ACS Sens.* **2018**, *3*, 1616−1621.
(47) Doldan, X.; Fagundez, P.; Cayota, A.; Laíz, J.; Tosar, J. P. *Anal. Chem.* **2016**, *88*, 10466−10473.
(48) Dong, H.; Chen, H.; Jiang, J.; Zhang, H.; Cai, C.; Shen, Q. *Anal. Chem.* **2018**, *90*, 4507−4513.
(49) Lamprecht, A. L.; Naujokat, S.; Margaria, T.; Steffen, B. *J. Biomed. Semant.* **2011**, *2*, S5.

DOI: 10.1021/acs.analchem.9b01950
Anal. Chem. 2019, 91, 10679−10686